The Nonoctahedral Structures of d^0, d^1, and d^2 Hexamethyl Complexes**

Martin Kaupp

Dedicated to Professor Hans-Georg von Schnering

Abstract: The homoleptic d^0 hexamethyl complexes $[M(CH_3)_6]^{2-}$ (M = Ti, Zr, Hf), $[M(CH_3)_6]^-$ (M = V, Nb, Ta), $[M(CH_3)_6]$ (M = Cr, Mo, W), and $[M(CH_3)_6]^+$ (M = Tc, Re) all prefer nonoctahedral structures derived from a trigonal prism. This was shown by density functional calculations which employed quasirelativistic effective-core potentials. The nonconventional structures are due to both improved σ bonding M – CH_3 interactions in nonoctahedral versus octahedral structures, and to core polarization. While most of the anions feature regular trigonal-prismatic equilibrium structures **B** of D_3 symmetry, the neutral and cationic species are distorted towards a C_3 symmetrical structure **A**, as found previously for $[W(CH_3)_6]$. The computed trends may be understood on the basis of energy denominators for second-order orbital interactions, and ligand – ligand repulsion. As both are increased by scalar relativistic effects in the 5d row, the 4d complexes exhibit the largest deviations from a regular prism. C_{3v} structures derived from an octahedron are generally less stable than the prismatic arrangements. This is also valid for the d^1 complexes $[Tc(CH_3)_6]$ and $[Re(CH_3)_6]$, and for the d^2 systems $[Ru(CH_3)_6]$ and $[Os(CH_3)_6]$. However, due to the additional electrons present, these species are predicted to favor regular rather than distorted prisms. NMR and IR spectroscopic parameters for the, as yet unknown, compound $[Os(CH_3)_6]$ are predicted to facilitate experimental characterization. The molecular and electronic structures of all the species are discussed with the help of natural population analyses.

Keywords: density functional calculations · hexamethyl complexes · nonoctahedral structures · transition metals

Introduction

Recently, independent quantum chemical[1] and low-temperature X-ray diffraction[2] studies have conclusively shown that the equilibrium structure of hexamethyltungsten, $[W(CH_3)_6]$, is a distorted trigonal prism (the WC_6 skeleton has C_{3v} symmetry, the overall computed symmetry is only C_3[1], see also ref. [3]). Previous studies had favored a regular prism,[4, 5] and prior to that an octahedral structure had been assumed.[6] As $[W(CH_3)_6]$ is an experimentally accessible,[4, 6] neutral homoleptic complex with small and simple monodentate ligands, it serves as the most spectacular prototype for a nonoctahedral hexacoordinate complex with a formal d^0 configuration. Other examples include the solid-state structure of the $[Zr(CH_3)_6]^{2-}$ ion (regular trigonal prismatic, with a D_{3h} skeleton)[7] or computed structures of the simple hexahydride $[WH_6]$ (distorted trigonal prismatic, C_{3v}) and related hydride model systems.[1, 5, 8, 9] During the course of the present study, X-ray crystallographical studies of the complex anions $[TaR_6]^-$ (R = Ph, CH_2Ph) were reported by Kleinhenz et al.[10] to have structures close to a regular trigonal prism. Extended solid-state structures with trigonal prismatic metal coordination are well known.[11] Among further nonoctahedral hexacoordinate structures of molecular d^0 complexes, those with chelating ligands (e.g. dithiolates) have been of considerable interest.[12] Some related d^0 – d^2 compounds may be of biological significance in the context of model compounds for oxomolybdenum enzymes.[13]

At a more general level, these unusual coordination arrangements fit well with other nonclassical low-symmetry structures of d^0 systems, such as bent dicoordinate,[14, 15] pyramidal tricoordinate,[16] or square pyramidal pentacoordinate[5, 17, 18] complexes of Group 2 through Group 5 metals and of the lanthanides.[19] Many computational studies have shown that the low-symmetry structures are favored by a maximization of metal d-orbital participation in σ bonding to the ligands, as well as by the polarization of the subvalence p shell of the metal [these two aspects are not strictly separable,[20] as

[*] Priv.-Doz. Dr. M. Kaupp
Max-Planck-Institut für Festkörperforschung
Heisenbergstrasse 1, D-70569 Stuttgart (Germany)
Fax: (+49) 711-689-1010
E-mail: kaupp@vsibm1.mpi-stuttgart.mpg.de

[**] Supporting information for this article is available on the WWW under http://www.wiley-vch.de/home/chemistry/ or from the author. The data contains the full Cartesian coordinates in Å for all optimized structures (16 Tables).

0947-6539/98/0409-1678 $ 17.50+.50/0

the valence $(n-1)$d orbitals and the semi-core $(n-1)$p orbitals for these early transition metals have very similar radial maxima]. In contrast, ligand–ligand repulsion and π bonding favor more symmetrical structures.

Do all d^0 hexamethyl complexes prefer nonoctahedral structures? Are they regular trigonal prismatic, like the anion in $[Li(tmed)]_2[Zr(CH_3)_6]$ (tmed = *N*,*N*,*N*′,*N*′-tetramethyl ethylenediamine),[7] or distorted like $[W(CH_3)_6]$?[1, 2] In order to gain a better understanding of the electronic effects that govern the structural preferences of these types of systems, we have now extended our computational study of $[W(CH_3)_6]$[1] to other valence-isoelectronic hexamethyl complexes: anionic: $[M(CH_3)_6]^{2-}$ (M = Ti, Zr, Hf), $[M(CH_3)_6]^-$ (M = V, Nb, Ta); neutral: $[M(CH_3)_6]$ (M = Cr, Mo, W); cationic: $[Tc(CH_3)_6]^+$, $[Re(CH_3)_6]^+$. We will also examine neutral complexes with a formal d^1 or d^2 configuration of the metal ($[M(CH_3)_6]$, M = Tc, Re, Ru, Os) to investigate the structural effects of additional electrons. Thus, for example, we show that the d^1 species $[Re(CH_3)_6]$ has a regular prismatic structure, in contrast to the conclusions drawn from a recent X-ray structure determination.[2] These studies also serve as a basis for the investigation of more complicated, heteroleptic compounds, which we have initiated.[21, 22] Moreover, we hope that our structural predictions will stimulate more experimental work in this area.

Abstract in German: *Die homoleptischen d^0-Hexamethyl-Komplexe $[M(CH_3)_6]^{2-}$ (M = Ti, Zr, Hf), $[M(CH_3)_6]^-$ (M = V, Nb, Ta), $[M(CH_3)_6]$ (M = Cr, Mo, W) und $[M(CH_3)_6]^+$ (M = Tc, Re) bevorzugen durchweg nichtoktaedrische, vom trigonalen Prisma abgeleitete Strukturen. Dies zeigen Dichtefunktional-Berechnungen mit quasirelativistischen Pseudopotentialen. Die nichtklassischen Strukturen gehen auf verbesserte M–CH_3 σ-Bindungen in den nichtoktaedrischen Strukturen und auf Rumpfpolarisation zurück. Während die meisten der anionischen Systeme regulär trigonal-prismatische Strukturen **B** mit D_3-Symmetrie aufweisen, sind die neutralen und die kationischen Spezies nach C_3-Symmetrie (**A**) verzerrt, wie bereits zuvor für $[W(CH_3)_6]$ gefunden. Die berechneten Trends werden durch die Betrachtung von Energie-Nennern für Orbitalwechselwirkungen in Störungstheorie zweiter Ordnung sowie durch die Ligand–Ligand-Abstoßung verständlich. Da beide durch skalar-relativistische Effekte in der 5d-Reihe erhöht werden, weisen die 4d-Komplexe die größte Tendenz zur Verzerrung der prismatischen Struktur auf. Vom Oktaeder abgeleitete C_{3v}-Strukturen **C** sind generell weniger stabil als die prismatischen Anordnungen. Dies gilt auch für die d^1-Komplexe $[Tc(CH_3)_6]$ und $[Re(CH_3)_6]$ sowie für die d^2-Systeme $[Ru(CH_3)_6]$ und $[Os(CH_3)_6]$. Aufgrund der zusätzlichen Elektronen werden diese Spezies jedoch als regulär trigonal-prismatisch vorhergesagt. NMR- und IR-spektroskopische Parameter für die bislang unbekannte Verbindung $[Os(CH_3)_6]$ werden zur Unterstützung einer experimentellen Charakterisierung angegeben. Die Strukturen und elektronischen Eigenschaften aller Komplexe werden mit Hilfe der natürlichen Populationsanalyse diskutiert.*

Computational details: In our previous study of $[W(CH_3)_6]$,[1] we found that the structural and energetic characteristics computed by density functional theory (DFT) with gradient-corrected exchange-correlation functionals are in excellent agreement with the results of more sophisticated post-Hartree–Fock treatments (MP2, CCSD, CCSD(T)). Therefore, throughout the present study we employed the more economical DFT methods, which employed Becke's exchange functional[23] and Perdew's correlation functional[24] (this combination of gradient-corrected functionals is often denoted as BP86). The basis sets correspond to basis A of ref. [1]. Thus, quasirelativistic small-core effective-core potentials (ECPs) and 6s5p3d valence basis sets[25] are used for the metals (for $[W(CH_3)_6]$ we also include results obtained with a nonrelativistic metal ECP[25b] for comparison). Carbon ECPs and DZP valence basis sets,[26] as well as a hydrogen DZ basis[27] are also the same as in ref. [1]. We note in passing that the use of ab initio derived ECPs in DFT applications is well validated for the core sizes employed here.[1, 28]

Following the experience with a larger set of possible structures for $[W(CH_3)_6]$,[1, 5] we have decided to compare the structures and energies for three stationary points on the $[M(CH_3)_6]^{(m)}$ potential energy surfaces (Figure 1): The distorted trigonal prismatic C_3-symmetric structure **A** (Figure 1a) corresponds to the equilibrium structure of $[W(CH_3)_6]$.[1, 2] The regular prismatic D_3 structure **B** (Figure 1b) is a low-lying transition state for the tungsten complex.[1] As a third alternative, the distorted octahedral C_{3v} arrangement **C** (Figure 1c) has been considered. For the dianions $[M(CH_3)_6]^{2-}$, the optimization of **C** converged to a D_{3d} symmetric structure, close to a regular octahedral framework. In all other cases, we expect regular octahedral structures to be considerably less favorable than structure **C**, as shown previously[1, 5] for $[W(CH_3)_6]$ (in many cases, SCF convergence in D_{3d} symmetry was difficult to achieve, and we have not attempted a systematic survey of these stationary points). Positive energies are calculated for those six occupied Kohn–Sham orbitals of the dianions $[M(CH_3)_6]^{2-}$ (M = Ti, Zr, Hf) with the highest energies. This indicates that the free dianions are probably not stable with respect to electron detachment. Nevertheless, we expect the structural results and computed relative energies to be meaningful, as the limited one-particle basis set does not allow the ejection of electrons from the system (this is confirmed by comparison with the experimental structure for $[Zr(CH_3)_6]^{2-}$, cf. below). Similar considerations are frequently used for anionic systems and should hold well, provided the negative charge is not too large.[29] The monoanions do not have positive occupied MO energies.

In the case of structure **C** for the d^2 systems $[Os(CH_3)_6]$ and $[Ru(CH_3)_6]$, it was not obvious from qualitative MO arguments, whether the ground state would be a closed-shell singlet or an open-shell triplet state, as the lowest unoccupied MO (LUMO) for the corresponding structures of the d^0 systems is a degenerate set of *e* symmetry; however, an a_1 MO is energetically almost degenerate as well (these three orbitals may be regarded as derived from a t_{2g} set at O_h symmetry). Therefore, both possibilities have been evaluated. However, it turned out that the singlet states were difficult to converge in DFT calculations. We thus resorted to Hartree–

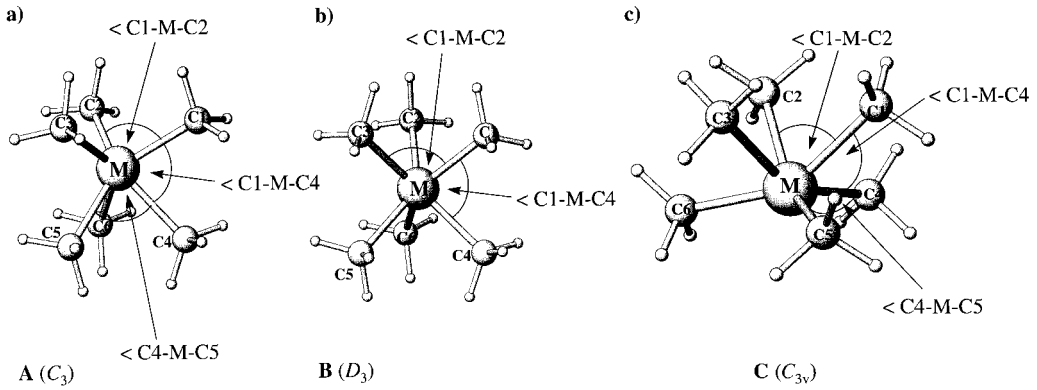

Figure 1. Atom labeling for the three $[M(CH_3)_6]^{(m)}$ structures considered. a) Distorted trigonal-prismatic C_3 structure **A**. b) Regular trigonal-prismatic D_3 structure **B**. c) Distorted octahedral C_{3v} structure **C**.

Fock calculations (which converge more easily, due to the larger band gap obtained), and used the Hartree–Fock optimized structures and MOs to start subsequent DFT calculations. The resulting DFT-optimized structures were close to the HF results. However, the energy of the highest occupied Kohn–Sham MO (HOMO) obtained was slightly higher than that of the LUMO. This does indicate difficulties with the correct description of these singlet states with a high-lying nonbonding HOMO by the present DFT calculations.[30] As the energies obtained for these singlet states are generally significantly above the triplet energies (which are themselves not competitive with structures **B**), we will in the following concentrate on the triplet results only.

All structures have been fully optimized within the given point group symmetry. The calculations were carried out with the Gaussian 94 and Gaussian 92/DFT programs.[31] Open-shell species (doublet $[Tc(CH_3)_6]$ and $[Re(CH_3)_6]$, and the triplet states of $[Ru(CH_3)_6]$ and $[Os(CH_3)_6]$ for structure **C**) were computed at the unrestricted (spin-polarized) Kohn–Sham level. Generally, the 'finegrid' option of the Gaussian programs was used for numerical integrations. In selected cases (see below), the nature of the stationary points was characterized by harmonic vibrational frequency analyses, by the use of numerical differentiation of analytical first energy derivatives. Natural population analyses[32] (NPA) used the built-in subroutines of the Gaussian packages.[31]

Table 1. Relative energies [kJ mol^{-1}] for different stationary points on the potential energy surfaces.[a]

Species	Distorted prism **A** (C_3)	Regular prism **B** (D_3)	Distorted octahedron **C** (C_{3v})
$[Ti(CH_3)_6]^{2-}$	–	0.0	+52.8[b]
$[Zr(CH_3)_6]^{2-}$	–	0.0	+65.8[b]
$[Hf(CH_3)_6]^{2-}$	–	0.0	+43.4[b]
$[V(CH_3)_6]^-$	–	0.0	+120.0
$[Nb(CH_3)_6]^-$	0.0	+0.8	+125.4
$[Ta(CH_3)_6]^-$	–	0.0	+130.1
$[Cr(CH_3)_6]$	0.0	+11.5	+98.6
$[Mo(CH_3)_6]$	0.0	+39.3	+110.3
$[W(CH_3)_6]$ (QR)	0.0	+24.6	+131.9
$[W(CH_3)_6]$ (NR)	0.0	+52.5	+103.3
$[Tc(CH_3)_6]^+$	0.0	+112.2	+90.3
$[Re(CH_3)_6]^+$	0.0	+93.0	+110.0
$[Tc(CH_3)_6]$[c]	–	0.0	+148.1
$[Re(CH_3)_6]$[c]	–	0.0	+169.5
$[Ru(CH_3)_6]$	–	0.0[d]	+136.3[e]
$[Os(CH_3)_6]$	–	0.0[d]	+160.4[e]

[a] Energies relative to the most stable structure (distorted trigonal prism **A** if observed, otherwise regular prism **B**). [b] Optimizations converged to D_{3d} symmetry. [c] Doublet states. [d] Closed-shell singlet states. [e] Triplet states.

Results and Discussion

A. Relative energies: Table 1 gives the relative energies obtained for the different stationary points. For all species, the distorted octahedral arrangements **C** are significantly higher in energy than structures **A** or **B** derived from the trigonal prism. Structure **C** is the most competitive for the d^0 dianions of Group 4 (a similar situation also pertains to simple hydride model systems[5, 8, 9]). Here the optimization converged to almost regular octahedral D_{3d} structures (cf. subsection B below), which are only $\approx 40-65$ kJ mol^{-1} above the preferred trigonal prismatic arrangements (D_3 structures **B**). In all other cases, structure **C** is considerably less stable. Thus, apparently all species studied here prefer structures derived from the trigonal prism rather than those derived from the octahedron. Harmonic vibrational frequency analyses give one imaginary frequency for structure **C** of $[Cr(CH_3)_6]$ and $[W(CH_3)_6]$. Previous optimizations of the latter species without symmetry or with C_3 symmetry, starting from structure **C**, converged back to structure **A**.[1] Seven imaginary frequencies are computed for the D_{3d} structure **C** of $[Hf(CH_3)_6]^{2-}$.

All dianions and two of the monoanions ($[V(CH_3)_6]^-$, $[Ta(CH_3)_6]^-$) definitely prefer regular trigonal-prismatic structures **B**, in agreement with the regular prismatic solid-state structures of $[Zr(CH_3)_6]^{2-}$,[7] $[TaPh_6]^-$,[10] and $[Ta(CH_2Ph)_6]^-$.[10] In contrast, a distortion to **A** is found for all neutral Group 6 species $[M(CH_3)_6]$ (M = Cr, Mo, W),[1, 2] and for the cations $[Tc(CH_3)_6]^+$ and $[Re(CH_3)_6]^+$. In these cases, **B** is a transition state, between 12 kJ mol^{-1} and 112 kJ mol^{-1} higher in energy than **A**. The same holds for $[Nb(CH_3)_6]^-$; however, here the energy gain upon distortion is only ≈ 0.8 kJ mol^{-1}, and the structural distortions are relatively small (see Section B). Apparently, in this case the potential energy surface for the 'inversion motion' **A** → **B** → **B**

0947-6539/98/0409-1680 $ 17.50+.50/0 *Chem. Eur. J.* **1998**, *4*, No. 9

is very shallow. Indeed, the negative force constant of the A2 symmetry inversion mode computed for **B** is only ≈ -0.02 mDyne Å^{-1} (imaginary frequency $\omega = i82$ cm^{-1}) in $[Nb(CH_3)_6]^-$, compared to about -0.25 mDyne Å^{-1} (imaginary frequency $\omega = i282$ cm^{-1}) and ≈ -1.04 mDyne Å^{-1} ($\omega = i745$ cm^{-1}) at the same level for $[W(CH_3)_6]$ and $[Re(CH_3)_6]^+$, respectively. Apparently, very recent X-ray diffraction studies give regular trigonal-prismatic structures for both $[Ta(CH_3)_6]^-$ and $[Nb(CH_3)_6]^-$.[33] This may indicate that the very small tendency of the niobium system to distort is too insignificant to be detectable in the solid state.

Optimizations in C_3 symmetry for the d^1 and d^2 systems $[M(CH_3)_6]$ (M = Tc, Re, Ru, Os) also lead to very slightly lower energies (by ≈ 0.7, 0.7, 2.5, and 1.9 kJ mol^{-1}, respectively) than those obtained in D_3 symmetry. However, here the structural deviations from **B** are negligible, and vibrational frequency analyses for **B** give no imaginary frequencies [the A2 'inversion' mode is computed to have a positive force constant of $+0.03$ mDyne Å^{-1} ($\omega = 114$ cm^{-1}) for $[Re(CH_3)_6]$, and of $+0.11$ mDyne Å^{-1} ($\omega = 278$ cm^{-1}) for $[Os(CH_3)_6]$. In these cases, the very shallow potential energy surfaces may be at the limits of accuracy for the numerical integrations of the exchange-correlation potential in the DFT calculations. In any case, the addition of electrons to formal d^0 species reduces the driving force towards distortion to the extent that the d^1 and d^2 species should be regarded as regular trigonal prismatic.

The present results for $[Re(CH_3)_6]$[1] disagree with the recent structure determination by Pfennig and Seppelt,[2] which gave preference to a distorted structure **A**, albeit with less deviations from **B** than found for $[W(CH_3)_6]$. Therefore, we have also optimized the structure of $[Re(CH_3)_6]$ at the MP2 level (with the same basis sets as in the DFT calculations). The MP2 structures, optimized in C_3 symmetry, are in excellent agreement with the DFT results and indicate no deviation from a regular prism. Meanwhile, a better refinement of the X-ray data for $[Re(CH_3)_6]$ has apparently been achieved,[33] which confirms the computed regular prism.

The barrier for the **A** → **B** → **A** inversion increases from $[Cr(CH_3)_6]$ to $[Mo(CH_3)_6]$ but decreases from $[Mo(CH_3)_6]$ to $[W(CH_3)_6]$. Similarly, the barrier is larger for $[Tc(CH_3)_6]^+$ than for $[Re(CH_3)_6]^+$ (note also the differences between $[Nb(CH_3)_6]^-$ and $[Ta(CH_3)_6]^-$). As the barrier for $[W(CH_3)_6]$ is larger with a nonrelativistic than with a quasirelativistic tungsten ECP (NR vs. QR, Table 1), its reduction from the 4d to the corresponding isoelectronic 5d complex is largely due to scalar relativistic effects. We expect this to be a general phenomenon. The largest barrier is thus found for the cationic 4d species $[Tc(CH_3)_6]^+$. The reasons for these trends are discussed in subsection C. Note that structure **C** is even less competitive for the $5d^0$ complexes than for their $4d^0$ analogues (except for the D_{3d} structure of $[Hf(CH_3)_6]^{2-}$), due to relativity (Table 1).

B. Structures: The main structural parameters for the different stationary points are summarized in Tables 2–4. The data given are restricted to the skeletal parameters. The hydrogen positions, and thus the finer details of the methyl group deformations (e.g. the slight twisting of the methyl groups away from D_{3h} symmetry in **A**, as well as agostic interactions), may be inferred from the optimized Cartesian coordinate sets

Table 2. Skeletal structure parameters computed for the distorted trigonal-prismatic minima (C_3, **A**).[a]

Species	r(M–C1)	r(M–C4)	∢(C1-M-C2)	∢(C4-M-C5)	∢(C1-M-C4)
$[Nb(CH_3)_6]^-$	2.253	2.268	90.2	79.8	77.3
$[Cr(CH_3)_6]$	2.029	2.108	93.7	76.0	77.6
$[Mo(CH_3)_6]$	2.136	2.206	97.3	74.7	75.5
$[W(CH_3)_6]$ (QR)[b]	2.147	2.209	95.6	75.6	76.2
$[W(CH_3)_6]$ (NR)	2.174	2.244	98.8	74.1	74.7
$[Tc(CH_3)_6]^+$	2.069	2.184	99.6	73.8	74.4
$[Re(CH_3)_6]^+$	2.079	2.190	98.7	74.0	75.0

[a] Distances [Å], angles [°]. See Figure 1a for atom labeling. [b] Average experimental results are:[2] r(M–C1) = 2.12 Å, r(M–C2) = 2.20 Å, C1-M-C2 = 95.4°, C4-M-C5 = 76.8°.

Table 3. Skeletal structure parameters computed for the regular trigonal-prismatic structures (D_3, **B**).[a]

Species	r(M–C)	∢(C1-M-C2)	∢(C1-M-C4)
$[Ti(CH_3)_6]^{2-}$	2.240	84.5	78.2
$[Zr(CH_3)_6]^{2-}$	2.397	85.0	77.4
$[Hf(CH_3)_6]^{2-}$	2.393	85.2	77.5
$[V(CH_3)_6]^-$	2.130	83.9	78.9
$[Nb(CH_3)_6]^-$	2.262	84.7	77.9
$[Ta(CH_3)_6]^-$	2.266	84.8	77.8
$[Cr(CH_3)_6]$	2.070	82.7	80.6
$[Mo(CH_3)_6]$	2.175	83.7	79.3
$[W(CH_3)_6]$ (QR)	2.181	84.6	78.1
$[W(CH_3)_6]$ (NR)	2.216	83.6	79.3
$[Tc(CH_3)_6]^+$	2.133	81.4	82.3
$[Re(CH_3)_6]^+$	2.137	83.1	80.1
$[Tc(CH_3)_6]$	2.141	83.0	80.1
$[Re(CH_3)_6]$	2.151	83.6	79.4
$[Ru(CH_3)_6]$	2.106	81.9	81.8
$[Os(CH_3)_6]$	2.121	82.3	81.2

[a] Distances [Å], angles [°]. See Figure 1b for atom labeling.

Table 4. Skeletal structure parameters computed for the distorted octahedral arrangements (C_{3v}, **C**).[a]

Species	r(M–C1)	r(M–C4)	∢(C1-M-C2)	∢(C4-M-C5)	∢(C1-M-C4)
$[Ti(CH_3)_6]^{2-}$[b]	2.257		92.6		87.3
$[Zr(CH_3)_6]^{2-}$[b]	2.424		92.0		87.8
$[Hf(CH_3)_6]^{2-}$[b]	2.420		92.2		87.8
$[V(CH_3)_6]^-$	2.204	2.089	81.2	111.2	80.9
$[Nb(CH_3)_6]^-$	2.312	2.233	78.7	113.5	79.8
$[Ta(CH_3)_6]^-$	2.308	2.255	80.7	109.3	82.6
$[Cr(CH_3)_6]$	2.188	1.981	80.0	115.2	77.8
$[Mo(CH_3)_6]$	2.257	2.107	77.3	116.8	76.7
$[W(CH_3)_6]$ (QR)	2.258	2.120	77.9	115.9	77.6
$[W(CH_3)_6]$ (NR)	2.290	2.151	76.7	117.6	75.8
$[Tc(CH_3)_6]^+$	2.244	2.047	76.7	117.4	76.1
$[Re(CH_3)_6]^+$	2.248	2.059	76.9	117.0	76.6
$[Tc(CH_3)_6]$	2.223	2.101	79.3	115.8	77.3
$[Re(CH_3)_6]$	2.237	2.118	79.3	114.9	78.3
$[Ru(CH_3)_6]$[c]	2.215	2.104	83.2	114.6	77.3
$[Os(CH_3)_6]$[c]	2.222	2.120	82.3	113.9	78.2

[a] Distances [Å], angles [°]. See Figure 1c for atom labeling. [b] Convergence to 'regular octahedral' D_{3d} structures. [c] Results for the triplet state.

given in the Supporting Information. We only note here in passing, that for structures **A** and **C**, (C-H)→M agostic interactions are apparent from the structural data for all complexes, comparable to those discussed previously for $[W(CH_3)_6]$.[1] Agostic interactions are less noticeable for structure **B**.[1] We also note that neither in C_3 nor in D_3 symmetry are the two trigonal faces of the prism required to be exactly eclipsed, that is to have a twist angle of 0°. However, the optimized structures are generally very close to the ideal prism, with twist angles around 2–3° (the largest twist of ≈7° is computed for structure **A** of $[Cr(CH_3)_6]$).

For the distorted trigonal prismatic structures **A** (Table 2), deviations from the regular prism may be judged by the difference between the M–C1 and M–C4 distances, and between the C1-M-C2 and C4-M-C5 angles (see Figure 1a). In general, the M–C1 distances corresponding to the expanded face of the prism (larger C1-M-C2 angles) are contracted compared to the M–C distances in the regular prismatic D_3 structures **B** (Table 3), whereas the M–C4 distances are longer. The magnitude of the distortion increases along the series $[Nb(CH_3)_6]^- << [Cr(CH_3)_6] < [W(CH_3)_6] < [Mo(CH_3)_6] < [Re(CH_3)_6]^+ < [Tc(CH_3)_6]^+$. With a nonrelativistic tungsten ECP (NR), the distortion for $[W(CH_3)_6]$ is calculated to be larger than that for $[Mo(CH_3)_6]$, consistent with the larger 'inversion' barrier (see above). While the angular distortion for the anion $[Nb(CH_3)_6]^-$ is still significant, the M–C distances on the two faces differ much less than for the other systems, consistent with the almost negligible barrier.

More general comparisons of vertical and horizontal periodic trends for bond lengths and angles are provided by the data for structure **B** in Table 3. As expected, the M–C distances decrease along a given row of the periodic table, from dianion to monoanion to neutral complex to cation. Similarly, the distances increase on descending a group. However, corresponding 4d and 5d complexes have very similar M–C distances, due to the well-known combined effects of relativity and shell-structure expansion (lanthanide contraction).[34] The angular structures for these regular trigonal-prismatic arrangements are very similar. The C1-M-C2 angles within a given trigonal face of the prism increase very slightly with increasing overall negative charge, and are very slightly reduced for the 3d systems. The M–C distances in the d^1 systems $[Tc(CH_3)_6]$ and $[Re(CH_3)_6]$ are larger than in the corresponding cations, but are contracted compared to $[Mo(CH_3)_6]$ and $[W(CH_3)_6]$, respectively. The distances in $[Ru(CH_3)_6]$ and $[Os(CH_3)_6]$ are still somewhat shorter. This is to be expected from the incomplete screening of nuclear charge by the nonbonding metal d-electrons. A slight decrease of the C1-M-C2 angles is seen along a d^0-d^1-d^2 series within a given row. The computational results for the dianion $[Zr(CH_3)_6]^{2-}$ agree excellently with the average values [r(Zr–C) = 2.38 Å, ∢(C1-Zr-C2) = 85.0°, ∢(C1-M-C4) = 77.4°] obtained by X-ray diffraction for the salt $[Li(t\text{-}med)]_2[Zr(CH_3)_6]$.[7] Similarly, the parameters computed for $[Ta(CH_3)_6]^-$ agree well with those found for the first coordination shell around tantalum in solid $[Li_4Br_3(Et_2O)_7][Ta(CH_2Ph)_6]$.[10]

The C_{3v}-distorted octahedral arrangements **C** (Table 4, Figure 1c) deviate strongly from regular octahedra, except for the dianionic systems which prefer regular D_{3d} structures (these in turn deviate only by a few degrees from ideal octahedral bond angles). The expanded face of the distorted structures is close to planarity (see C4-M-C5 angles!). In all cases, the shorter M–C distances belong to this expanded face of the octahedron, similar to the situation for structure **A** (see above), in notable contrast to the structures of simple hexahydride model systems (in the hydride systems, the shorter M–H distances are generally connected to the compressed angles).[1, 5, 8, 9] While distortion from structure **B** to structure **A** is restricted mainly to the neutral and cationic d^0 systems (see above), the computed structures **C** deviate rather significantly from regular octahedra for all species, except for the dianions. This includes the d^1 and d^2 systems, which are almost as distorted as their d^0 counterparts.

C. Bonding analyses: Tables 5–7 summarize the main results of natural population analyses (NPA) for the different nuclear arrangements. The metal charges are generally much lower and the d populations are larger than those implied by a formal d^0 (or d^1, d^2) configuration and by the corresponding formal oxidation state. As expected, this covalent bonding character becomes more notable as one moves to the right in a given row of the periodic table (e.g. from $[Hf(CH_3)_6]^{2-}$ to $[Re(CH_3)_6]^+$). Thus, while the dianions still exhibit large negative charges on the methyl ligands, the charges may even be slightly positive for the hypothetical $[Tc(CH_3)_6]^+$ and $[Re(CH_3)_6]^+$. This is significant in the context of ligand–ligand repulsive interactions (see below).

For any of the three structures, the 5d complex of a given group exhibits the largest metal charge (Tables 5–7). As shown by the comparison of the quasirelativistic and nonrelativistic ECP results (QR vs. NR) for $[W(CH_3)_6]$, this is largely due to the well-known relativistic destabilization of the 5d orbitals,[34] which facilitates charge transfer. This relativistically increased bond ionicity is expected to be a

Table 5. NPA charges Q and metal populations for the C_3 structures **A**.[a]

Species	Q(M)	s(M)	p(M)	d(M)	Q(C1)	Q(C4)	Q(CH$_3$)1	Q(CH$_3$)4
$[Nb(CH_3)_6]^-$	+1.310	0.405	0.037	3.275	−1.069	−1.009	−0.400	−0.369
$[Cr(CH_3)_6]$	+0.829	0.382	0.020	4.791	−0.897	−0.783	−0.167	−0.111
$[Mo(CH_3)_6]$	+0.793	0.406	0.021	4.826	−0.907	−0.790	−0.161	−0.104
$[W(CH_3)_6]$ (QR)	+1.148	0.427	0.012	4.370	−0.982	−0.868	−0.215	−0.168
$[W(CH_3)_6]$ (NR)	+0.824	0.384	0.011	4.812	−0.905	−0.792	−0.166	−0.108
$[Tc(CH_3)_6]^+$	+0.465	0.413	0.051	6.125	−0.743	−0.651	+0.072	+0.106
$[Re(CH_3)_6]^+$	+0.804	0.501	0.017	5.707	−0.831	−0.713	+0.012	+0.052

[a] The charges and overall populations do not match exactly, as the depletion of some metal semi-core orbitals has been neglected.

0947-6539/98/0409-1682 $ 17.50+.50/0 *Chem. Eur. J.* **1998**, *4*, No. 9

Table 6. NPA charges Q and metal populations for the D_3 structures **B**.[a]

Species	Q(M)	s(M)	p(M)	d(M)	Q(C)	Q(CH_3)
$[Ti(CH_3)_6]^{2-}$	+1.399	0.402	0.130	2.082	−1.125	−0.566
$[Zr(CH_3)_6]^{2-}$	+1.581	0.418	0.115	1.907	−1.177	−0.596
$[Hf(CH_3)_6]^{2-}$	+1.863	0.461	0.068	1.607	−1.224	−0.644
$[V(CH_3)_6]^-$	+1.243	0.379	0.035	3.360	−1.008	−0.373
$[Nb(CH_3)_6]^-$	+1.356	0.406	0.039	3.224	−1.051	−0.393
$[Ta(CH_3)_6]^-$	+1.752	0.467	0.030	2.699	−1.127	−0.460
$[Cr(CH_3)_6]$	+0.979	0.380	0.023	4.637	−0.876	−0.164
$[Mo(CH_3)_6]$	+1.059	0.413	0.026	4.535	−0.914	−0.177
$[W(CH_3)_6]$ (QR)	+1.362	0.490	0.014	4.126	−0.981	−0.227
$[W(CH_3)_6]$ (NR)	+1.129	0.394	0.019	4.473	−0.924	−0.189
$[Tc(CH_3)_6]^+$	+0.819	0.395	0.027	5.801	−0.779	+0.030
$[Re(CH_3)_6]^+$	+1.106	0.520	0.024	5.388	−0.854	−0.018
$[Tc(CH_3)_6]$	+0.681	0.426	0.025	5.903	−0.824	−0.113
$[Re(CH_3)_6]$	+0.933	0.507	0.022	5.571	−0.883	−0.156
$[Ru(CH_3)_6]$	+0.319	0.429	0.021	7.259	−0.751	−0.053
$[Os(CH_3)_6]$	+0.566	0.518	0.013	6.916	−0.801	−0.095

[a] The charges and overall populations do not match exactly, as the depletion of some metal semi-core orbitals has been neglected.

correspondingly shorter ligand–ligand distances involved. This is also borne out by the computed structures and energies (Tables 1–4).

Following a qualitative second-order perturbation theory argument for orbital mixing upon distortion,[38] the driving force for a symmetry lowering should be inversely proportional to the energy difference between the relevant orbitals. Table 8 relates the inverse of the HOMO–LUMO energy differences ($1/\Delta\varepsilon$) for structures **B** of the d^0 systems to the **A** → **B** → **A** inversion barrier ΔE. If we restrict ourselves to the 4d and 5d species, there is a rough correspondence between $1/\Delta\varepsilon$ and ΔE, consistent with arguments based on second-order orbital mixing.[5, 8, 38] The greater importance of ligand–ligand repulsion for the 3d systems may be inferred from the fact that the barrier height is generally lower than expected from the comparison of $1/\Delta\varepsilon$ to the corresponding 4d and 5d complexes. Relativistic effects do not only increase the bond ionicity in $[W(CH_3)_6]$ (see Tables 5–7) but also the HOMO–LUMO gap in **B** (Table 8). This reduces the barrier height

Table 7. NPA charges Q and metal populations for C_{3v} structures **C**.[a]

Species	Q(M)	s(M)	p(M)	d(M)	Q(C1)	Q(C4)	Q(CH_3)1	Q(CH_3)4
$[Ti(CH_3)_6]^{2-}$[b]	+1.647	0.429	0.170	1.758	−1.187		−0.608	
$[Zr(CH_3)_6]^{2-}$[b]	+1.990	0.452	0.126	1.438	−1.266		−0.669	
$[Hf(CH_3)_6]^{2-}$[b]	+2.204	0.495	0.067	1.140	−1.295		−0.840	
$[V(CH_3)_6]^-$	+1.168	0.372	0.044	3.433	−0.909	−1.049	−0.358	−0.381
$[Nb(CH_3)_6]^-$	+1.187	0.409	0.048	3.387	−0.926	−1.074	−0.330	−0.400
$[Ta(CH_3)_6]^-$	+1.773	0.496	0.037	2.659	−1.056	−1.191	−0.436	−0.487
$[Cr(CH_3)_6]$	+0.654	0.345	0.016	5.009	−0.738	−0.851	−0.112	−0.108
$[Mo(CH_3)_6]$	+0.629	0.378	0.018	5.022	−0.738	−0.864	−0.085	−0.125
$[W(CH_3)_6]$ (QR)	+1.037	0.469	0.009	4.500	−0.809	−0.967	−0.143	−0.201
$[W(CH_3)_6]$ (NR)	+0.658	0.361	0.014	5.008	−0.742	−0.859	−0.089	−0.129
$[Tc(CH_3)_6]^+$	+0.397	0.380	0.013	6.262	−0.623	−0.716	+0.102	+0.099
$[Re(CH_3)_6]^+$	+0.681	0.474	0.010	5.863	−0.662	−0.803	+0.067	+0.037
$[Tc(CH_3)_6]$	+0.518	0.395	0.021	6.106	−0.723	−0.835	−0.065	−0.106
$[Re(CH_3)_6]$	+0.785	0.491	0.019	5.741	−0.765	−0.911	−0.100	−0.162
$[Ru(CH_3)_6]$[c]	+0.527	0.413	0.022	7.066	−0.734	−0.824	−0.071	−0.105
$[Os(CH_3)_6]$[c]	+0.742	0.519	0.017	6.749	−0.765	−0.885	−0.097	−0.151

[a] The charges and overall populations do not match exactly, as the depletion of some metal semi-core orbitals has been neglected. [b] Convergence to 'regular octahedral' D_{3d} structures. [c] Results for the triplet state.

general phenomenon for early 5d complexes in high formal oxidation states. We strongly suspect that it may be responsible for the generally higher tendency of 5d, as compared to 4d complexes, to aggregate in the condensed phase (e.g. Re_2O_7 is a polymeric solid,[35] whereas Tc_2O_7 features monomeric molecular units in its crystal structure[36]), or for the larger Lewis acidity of the 5d compared to 4d complexes in high oxidation states[37] (of course the larger ionicity also contributes to the larger overall stability of higher oxidation states in the 5d series[34a]). In the present context, the larger bond ionicity leads to larger ligand–ligand repulsion for the 5d complexes than for the corresponding 4d species. As a consequence, the 5d systems exhibit a smaller tendency to distort from the regular prism **B** to structure **A** (compare $[Re(CH_3)_6]^+$ vs. $[Tc(CH_3)_6]^+$, $[W(CH_3)_6]$ vs. $[Mo(CH_3)_6]$, or $[Ta(CH_3)_6]^-$ vs. $[Nb(CH_3)_6]^-$). On the other hand, we may also expect the 3d species to exhibit larger ligand–ligand repulsion than the 4d complexes, due to the significantly smaller metal radii, and to the even further for this and the other 5d complexes (compared to the 4d systems).

We note that structures **C** exhibit the lowest metal charges and the largest metal d populations for a given complex (except for the d^2 complexes and for the D_{3d} structures of the dianions, see Table 7). If maximization of the d population

Table 8. Computed HOMO and LUMO orbital energies (au)[a] for structure **B** compared to the **A**–**B**–**A** activation barrier (kJ mol^{-1}).

Species	ε(HOMO) (a_2)	ε(LUMO) (a_1)	$\Delta\varepsilon$	$1/\Delta\varepsilon$	ΔE(**B** − **A**)[b]
$[Cr(CH_3)_6]$	−0.216	−0.165	0.051	19.6	11.5
$[Mo(CH_3)_6]$	−0.206	−0.159	0.047	21.3	39.3
$[W(CH_3)_6]$ (QR)	−0.207	−0.145	0.052	19.2	24.6
$[W(CH_3)_6]$ (NR)	−0.202	−0.159	0.043	23.3	52.5
$[Tc(CH_3)_6]^+$	−0.401	−0.381	0.020	50.0	112.2
$[Re(CH_3)_6]^+$	−0.400	−0.375	0.025	40.0	93.0
$[V(CH_3)_6]^-$	−0.030	+0.055	0.085	11.8	–
$[Nb(CH_3)_6]^-$	−0.027	+0.059	0.086	11.6	0.8
$[Ta(CH_3)_6]^-$	−0.029	+0.074	0.103	9.7	–

[a] Kohn–Sham orbital energies. [b] See Table 1.

were the only criterion of stability, structure **C** should be the most stable one. Evidently, as we argued previously for $[W(CH_3)_6]$,[1] structure **C** must exhibit strong ligand–ligand repulsion, which increases as the complex distorts away from a regular octahedron to increase the d-orbital participation in σ-bonding (note that the D_{3d} structures for the dianions exhibit very low d populations and large metal charges). This makes the (strongly) distorted octahedral structures **C** less competitive with the arrangements based on a trigonal prism. As a general feature, the methyl groups on the expanded face of the distorted octahedron exhibit larger negative charges than those on the compressed side. Correspondingly, hybridization analyses of the corresponding natural localized molecular orbitals show more covalency and larger d-orbital participation on the compressed side.

Similarly, structures **A** have smaller negative charges and larger metal–ligand covalency (Table 5) for those methyl groups which are on the compressed side of the distorted trigonal prism (methyl groups 4–6, see Figure 1a). In general, distortion from **B** to **A** reduces the positive metal charges, in agreement with the notion of a general maximization of covalent σ bonding. The distortion particularly reduces the negative charges of the methyl groups on the compressed side, as these start to interact with a metal hybrid orbital formed from the d_z^2 orbital (mainly involved in the LUMO in structure **B**) and the p_z orbital. The charges of the methyl groups on the expanded side (C1–C4) change very little upon distortion.

For the d^1 and d^2 systems, the MO analysis of structure **B** confirms that the extra nonbonding electron(s) populate(s) a metal d_z^2-type orbital, with some additional small coefficients at the hydrogen atoms. This result is consistent with previous qualitative MO arguments.[1, 5, 8, 9] Evidently, this extra d_z^2 occupation quenches the tendency towards a low-symmetry **B**→**A** distortion, making the regular trigonal-prismatic structure **B** the most favorable arrangement. Compared to the d^0 cations $[M(CH_3)_6]^+$ (M = Tc, Re), the positive metal charges of the corresponding neutral d^1 systems are reduced much less than by one whole electronic charge (by ≈0.15 e when comparing structure **B** for both cations and neutral complexes). Thus, some rearrangement of charge towards the ligands takes place upon reduction, in spite of the dominant d_z^2 character of the singly occupied MO (SOMO; cf. ligand charges in Table 6). The NPA metal charges of the d^2 systems $[M(CH_3)_6]$ (M = Ru, Os) are also still appreciably positive (Table 6).

Gibson et al. have previously attempted to assign the EPR spectrum of $[Re(CH_3)_6]$ on the basis of octahedral symmetry.[39] To explain the observation of an EPR spectrum for this molecule (in contrast to the absence of EPR signals for the octahedral ReF_6, dynamically distorted by Jahn–Teller effects), they assumed that the degeneracy of the t_{2g} singly occupied MO had been lifted by spin-orbit coupling. In spite of this, no satisfactory fit of the electronic g tensor was achieved.[39] The trigonal-prismatic D_3 structure found here evidently allows a much easier rationalization of the EPR spectrum, as the unpaired electron occupies a nondegenerate a_1 MO. Similar considerations apply to the interpretation of the photoelectron spectra of $[Re(CH_3)_6]$ and $[W(CH_3)_6]$.[6c]

D. NMR and IR spectroscopic parameters for $[Os(CH_3)_6]$: While several of the prismatic d^0 systems discussed here, as well as the d^1 system $[Re(CH_3)_6]$, have now been experimentally investigated,[2, 4, 6, 7, 10, 33] the diselenolate complex $[W(Se_2(COOCH_3)_2)_3]^{2-}$[40] appears to be the only structurally characterized example of a molecular nonoctahedral system with a clear d^2 configuration (d^2 configurations have sometimes been assumed for dithiolene ligands, but due to the delocalized nature of bonding, the actual d configuration in these systems is not well defined[12, 13]). Therefore, the as yet unknown, simple trigonal prismatic hexamethyl complexes $[Ru(CH_3)_6]$ and $[Os(CH_3)_6]$ appear to be very interesting targets for experimental studies. This is particularly valid for the osmium complex, which should be the more stable species. Therefore, we present quantum chemical predictions of NMR chemical shifts, as well as IR frequencies and intensities, that will hopefully facilitate the experimental characterization.

The ^{13}C and ^1H chemical shieldings for the D_3 structures **B** have been calculated at the SOS-DFPT-IGLO level,[41] with the deMon-NMR program,[41, 42] using the same metal ECPs and valence basis sets as in the optimizations, but with IGLO-II all-electron basis sets[43] on C and H. All other computational parameters have already been detailed for $[W(CH_3)_6]$.[1] The calculations for $[Os(CH_3)_6]$ give a ^{13}C NMR shift of $\delta = +67.5$, and a ^1H shift of $\delta = +2.2$ (average for nonequivalent hydrogen atoms in D_3 symmetry), both relative to TMS. The corresponding shifts for $[Ru(CH_3)_6]$ are $\delta = +72.3$ and $+2.4$, respectively.

Our previously computed ^{13}C shifts at the same level for $[W(CH_3)_6]$ were $\delta = +53.3$ and $+71.3$ for the nonequivalent sets of carbon atoms in structure **A** (av $\delta = 62.3$). This is somewhat too low compared to the average experimental value of $\delta = 83.1$. The lower computed shifts for these types of systems should be largely due to systematic errors of the computational method.[1, 44] Thus, we also suspect that the ^{13}C shifts for the two d^2 systems may be higher than the computed values by roughly 20 ppm, which places our best estimates slightly below or above $\delta = 90$ for $[Os(CH_3)_6]$ and $[Ru(CH_3)_6]$, respectively. For the dianion $[Zr(CH_3)_6]^{2-}$, our calculations (structure **B**) give a ^{13}C shift of $\delta = 23.4$, which is in somewhat better agreement with the experimental value of $\delta = 32.0$.[7] The small deviation from the experimental value and the relatively low shift are both consistent with a relatively large HOMO–LUMO energy gap for the dianion.

Figure 2 shows the predicted IR spectrum for $[Os(CH_3)_6]$, obtained by convoluting the computed harmonic vibrational frequencies and intensities for structure **B** with Lorenzians of half-width = 10 cm^{-1}. Compared to the previously computed spectrum for $[W(CH_3)_6]$ at the same level (for structure **A**),[1] the predicted spectrum for the osmium complex is considerably simpler, which is partly due to the higher symmetry. Most notably, however, there is very little intensity in the M–C stretching region around 500–550 cm^{-1}. Figure 3 shows the corresponding computed spectrum for the d^1 complex $[Re(CH_3)_6]$, which agrees well with the experimental data.[45] The structure of the spectrum is very similar to that of the osmium complex, except for the

0947-6539/98/0409-1684 $ 17.50+.50/0 *Chem. Eur. J.* **1998**, *4*, No. 9

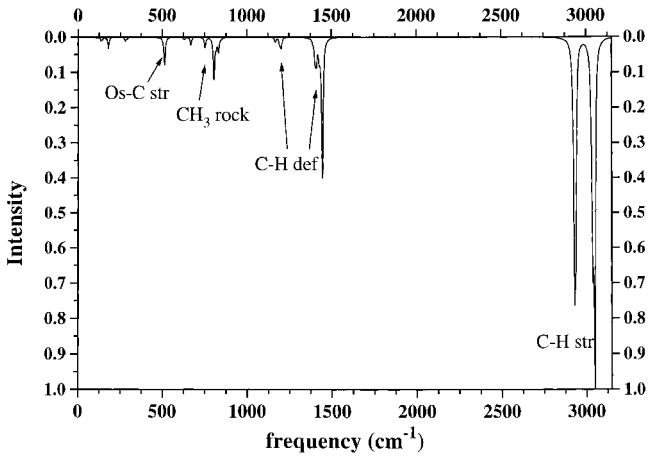

Figure 2. Simulated IR spectrum for $[Os(CH_3)_6]$ (D_3 structure **B**). The calculated harmonic vibrational frequencies and intensities have been convoluted by Lorenzians of half-width 10 cm^{-1}. Intensities have been scaled to that of the most intense band. Assignments are indicated by arrows.

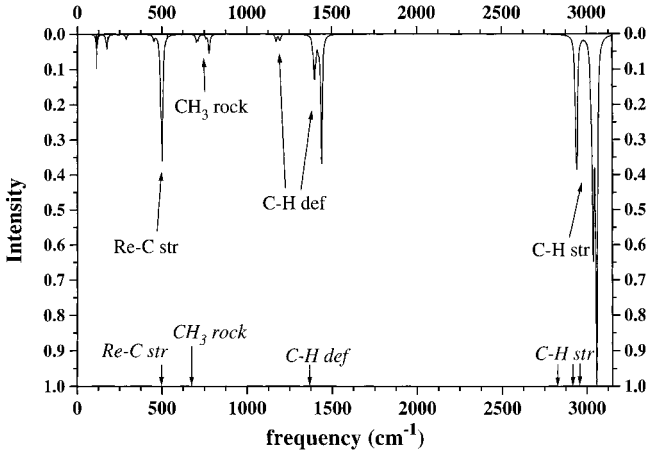

Figure 3. Simulated IR spectrum for $[Re(CH_3)_6]$ (D_3 structure **B**). Computational assignments in normal letters, experimental assignments from ref. [45] at the bottom of the diagram in italics.

somewhat larger intensity in the M–C stretching region. The decrease in M–C stretching intensity along the series $[W(CH_3)_6] > [Re(CH_3)_6] > [Os(CH_3)_6]$ is readily explained by the significant decrease in M–C bond polarity along the same series (cf. computed charges in Tables 5 and 6).

Conclusions

All homoleptic d^0, d^1, and d^2 hexamethyl complexes studied here by quantum chemical calculations prefer coordination polyhedra derived from a trigonal prism rather than from an octahedron. Consistent with previous results for $[W(CH_3)_6]$,[1, 2] the isoelectronic $[Cr(CH_3)_6]$ and $[Mo(CH_3)_6]$ compounds feature trigonal-prismatic structures distorted towards C_3 symmetry. Even more strongly distorted C_3 structures are predicted for the hypothetical cations $[Tc(CH_3)_6]^+$ and $[Re(CH_3)_6]^+$. In contrast, the dianions $[M(CH_3)_6]^{2-}$ (M = Ti, Zr, Hf) and the monoanions $[M(CH_3)_6]^-$ (M = V, Ta) have regular prismatic D_3 structures, consistent with experimental results for the $[Zr(CH_3)_6]^{2-}$ ion,[7] with X-ray results for $[TaR_6]^-$ (R = phenyl, tolyl),[10] and with a very recent X-ray study of $[Ta(CH_3)_6]^-$.[33] For $[Nb(CH_3)_6]^-$ the calculations indicate very slight deviations from the regular prism, with a shallow potential for the 'inversion' motion.

A distortion of the prism is only preferable when the increased repulsion between the ligands, or between ligand orbitals and nonbonding metal orbitals (for the d^1 and d^2 systems), is overcome to a significant extent by the electronic driving forces for distortion (mainly the improved metal d-orbital participation in σ bonding to the ligands, possibly also the polarization of the metal semi-core p shell). As a negative molecular charge is mainly concentrated on the ligands, the anions have the least tendency to distort, whereas the cations $[Tc(CH_3)_6]^+$ and $[Re(CH_3)_6]^+$ show the largest covalency and thus the largest distortion. Within a given group, the tendency to distort increases from the 3d to the 4d complex but decreases to the 5d complex, such that it is largest for the 4d species. The smaller distortions for the 5d species are due to the scalar relativistic expansion of the 5d orbitals, which, for example, leads to increased bond ionicity and thus to larger ligand–ligand repulsion. Apart from these electrostatic considerations, the relativistic increase of the energy gap between the relevant MOs (those that mix upon symmetry lowering) also reduces the preference for distortion.

The addition of electrons to the d_z^2-type LUMO of the regular prismatic structure **B** (cf. qualitative MO diagram in refs. [5, 8a]) reduces the tendency to distort towards structure **A**. Thus, the d^1 complexes $[Tc(CH_3)_6]$ and $[Re(CH_3)_6]$ and the d^2 species $[Ru(CH_3)_6]$ and $[Os(CH_3)_6]$ apparently prefer regular prismatic structures **B**. The discrepancy between the computational prediction for $[Re(CH_3)_6]$[1] and a previous experimental study giving a distorted structure[2] appears to have been settled in favor of the regular prism.[33] Of course, the very shallow potential for the 'inversion' motion **A** → **B** → **A** in this species has to be kept in mind. Even for the, as yet experimentally unknown, d^2 systems $[Ru(CH_3)_6]$ and $[Os(CH_3)_6]$, a structure **C**, derived from an octahedron, is not competitive with the trigonal prismatic arrangement **B**. NMR and IR spectroscopic predictions have been made for the $[Os(CH_3)_6]$ molecule to facilitate its experimental characterization.

The nonoctahedral structural preferences found here for all of the d^0 hexamethyl complexes should be contrasted to the more conventional, regular octahedral d^0 systems with electronegative π-donating ligands, for example $[MX_6$ (M = Cr, Mo, W; X = halogen, OR, NR_2). One may expect that mixed-ligand systems $[MX_nY_{6-n}]$ ($n = 1-5$) featuring both π-donor ligands Y and pure σ-donor ligands X, may at some n exhibit a change in preference from octahedral to trigonal prismatic structures. This notion is indeed confirmed by first exploratory calculations.[22]

Acknowledgments: I thank Prof. Dr. K. Seppelt (FU Berlin) for communicating results of his parallel, independent experimental investigations[33] prior to publication, and Dr. B. Farid (Stuttgart) for helpful

discussions. I am grateful to the Deutsche Forschungsgemeinschaft (DFG) for a 'Habilitationsstipendium' (1995–1997), and to Prof. Dr. H. G. von Schnering (Max-Planck-Institut Stuttgart) for his generous support.

Received: December 15, 1997
Revised version: March 27, 1998 [F932]

[1] M. Kaupp, *J. Am. Chem. Soc.* **1996**, *118*, 3018.
[2] V. Pfennig, K. Seppelt, *Science* **1996**, *271*, 626.
[3] C. R. Landis, T. Cleveland, T. K. Firman, *J. Am. Chem. Soc.* **1995**, *117*, 1859; C. R. Landis, T. Cleveland, T. K. Firman, *Science* **1996**, *272*, 179.
[4] A. Haaland, A. Hammel, K. Rypdal, H. V. Volden, *J. Am. Chem. Soc.* **1990**, *112*, 4547.
[5] S. K. Kang, H. Tang, T. A. Albright, *J. Am. Chem. Soc.* **1993**, *115*, 1971.
[6] a) A. L. Galver, G. Wilkinson, *J. Chem. Soc. Dalton Trans.* **1976**, 2235; b) A. J. Shortland, G. Wilkinson, *ibid.* **1973**, 872; c) J. C. Green, D. R. Lloyd, L. Galyer, K. Mertis, G. Wilkinson, *ibid.* **1978**, 1403.
[7] P. M. Morse, G. S. Girolami, *J. Am. Chem. Soc.* **1989**, *111*, 4114 (this was the first example of a trigonal prismatic d^0 complex with simple unidentate ligands).
[8] a) S. K. Kang, T. A. Albright, P. Eisenstein, *Inorg. Chem.* **1989**, *28*, 1611; b) A. Demolliens, Y. Jean, O. Eisenstein, *Organometallics* **1986**, *5*, 1457.
[9] See for example: a) M. Shen, H. F. Schaeffer, III, H. Partridge, *J. Chem. Phys.* **1993**, *98*, 508; b) V. Jonas, G. Frenking, J. Gauss, *Chem. Phys. Lett.* **1992**, *194*, 109; c) D. G. Musaev, O. P. Charkin, *Sov. J. Coord. Chem.* **1989**, *15*, 102; d) A. Zyubin, D. G. Musaev, O. P. Charkin, *Russ. J. Inorg. Chem.* **1992**, *37*, 1214; e) P. E. M. Siegbahn, M. R. A. Blomberg, *J. Am. Chem. Soc.* **1993**, *115*, 4191.
[10] S. Kleinhenz, M. Schubert, K. Seppelt, *Chem. Ber.* **1997**, *130*, 903.
[11] See for example: B. Huisman, R. de Jonge, C. Haas, F. Jellinek, *J. Solid State Chem.* **1971**, *3*, 56, and references therein. For a very recent example, see: M. Lulei, J. D. Corbett, *Angew. Chem.* **1995**, *107*, 2463; *Angew. Chem. Int. Ed. Engl.* **1995**, *34*, 2262.
[12] Compare for example: R. Eisenberg, *Prog. Inorg. Chem.* **1970**, *12*, 295, and references therein.
[13] See for example: A. Cervilla, J. A. Ramirez, E. Llopis, P. Palanca, *Inorg. Chem.* **1993**, *32*, 2085, and references therein.
[14] a) M. Kaupp, P. von R. Schleyer, H. Stoll, H. Preuss, *J. Chem. Phys.* **1991**, *94*, 1360; b) M. Kaupp, P. von R. Schleyer, H. Stoll, H. Preuss, *J. Am. Chem. Soc.* **1991**, *113*, 6012; c) L. Seijo, Z. Barandiaran, S. Huzinaga, *J. Chem. Phys.* **1991**, *94*, 762; d) M. Kaupp, P. von R. Schleyer, *J. Am. Chem. Soc.* **1992**, *114*, 491; e) M. Kaupp, P. von R. Schleyer, H. Stoll, M. Dolg, *ibid.* **1992**, *114*, 8202; f) M. Kaupp, O. P. Charkin, P. von R. Schleyer, *Organometallics* **1992**, *11*, 2767.
[15] a) J. S. Ghotra, M. B. Hursthouse, A. J. Welch, *J. Chem. Soc. Chem. Commun.* **1973**, 669; b) R. A. Andersen, D. H. Templeton, A. Zalkin, *Inorg. Chem.* **1978**, *17*, 2317. c) C. Eaborn, S. A. Hawkes, P. B. Hitchcock, J. D. Smith, *J. Chem. Soc. Chem. Commun.* **1997**, 1961.
[16] a) C. A. Jolly, D. S. Marynick, *Inorg. Chem.* **1989**, *28*, 2893; b) C. W. Bauschlicher, Jr., M. Sodupe, H. Partridge, *J. Chem. Phys.* **1992**, *96*, 4453; c) M. Kaupp, P. von R. Schleyer, *J. Phys. Chem.* **1992**, *96*, 7316; d) P. E. M. Siegbahn, *ibid.* **1993**, *97*, 9096.
[17] C. Pulham, A. Haaland, A. Hammel, K. Rypdal, H. P. Verne, H. V. Volden, *Angew. Chem.* **1992**, *104*, 1534; *Angew. Chem. Int. Ed. Engl.* **1992**, *31*, 1464.
[18] T. A. Albright, H. Tang, *Angew. Chem.* **1992**, *104*, 1532; *Angew. Chem. Int. Ed. Engl.* **1992**, *31*, 1462.
[19] C. Eaborn, P. B. Hitchcock, K. Izod, J. D. Smith, *J. Am. Chem. Soc.* **1994**, *116*, 12071; C. Eaborn, P. B. Hitchcock, K. Izod, Z.-R. Lu, J. D. Smith, *Organometallics*, **1996**, *15*, 4783.
[20] M. Kaupp, *Dissertation*, Universität Erlangen-Nürnberg (Germany) **1992**.
[21] Thus, for example, d^0 $[MXR_4]$ complexes (X = π-donor ligand, R = σ-donor ligand) exhibit very unusual structural preferences (M. Kaupp, *Chem. Eur. J.* in press). Similar considerations are valid for $[MX_2R_3]$ systems (T. R. Ward, H.-B. Bürgi, F. Gillardoni, J. Weber, *J. Am. Chem. Soc.* **1997**, *119*, 11974).
[22] Mixed complexes $[WX_n(CH_3)_{6-n}]$ (X = F, Cl; $n = 1-5$) are predicted computationally to exhibit a gradual change in the preference from a prismatic to a octahedral structure as n increases (M. Kaupp, unpublished results).
[23] A. D. Becke, *Phys. Rev. A* **1988**, *38*, 3098.
[24] J. P. Perdew, *Phys. Rev. B* **1986**, *33*, 8822.
[25] M. Dolg, U. Wedig, H. Stoll, H. Preuß, *J. Chem. Phys.* **1987**, *86*, 866; D. Andrae, U. Häußermann, M. Dolg, H. Stoll, H. Preuss, *Theor. Chim. Acta* **1990**, *77*, 123.
[26] A. Bergner, M. Dolg, W. Küchle, H. Stoll, H. Preuss, *Mol. Phys.* **1993**, *80*, 1431.
[27] N. Godbout, D. R. Salahub, J. Andzelm, E. Wimmer, *Can. J. Chem.* **1992**, *70*, 560.
[28] a) C. van Wüllen, *Int. J. Quant. Chem.* **1996**, *58*, 147; b) T. V. Russo, R. L. Martin, P. J. Hay, *J. Phys. Chem.* **1995**, *99*, 17085; c) For further examples in the context of NMR chemical shift calculations see: M. Kaupp, V. G. Malkin, O. L. Malkina, D. R. Salahub, *Chem. Phys. Lett.* **1995**, *235*, 382; M. Kaupp, V. G. Malkin, O. L. Malkina, D. R. Salahub, *Chem. Eur. J.* **1996**, *2*, 24; M. Kaupp, *ibid.* **1996**, *2*, 348.
[29] For a more detailed discussion, see for example: P. Pyykkö, Y. Zhao, *J. Phys. Chem.* **1990**, *94*, 7753.
[30] This particular structure and state may not be pure-state v-representable. For discussions of the v-representability problem, see for example: *Density Functional Theory of Atoms and Molecules*, R. G. Parr, W. Yang, Oxford University Press, Oxford **1989**; *Density Functional Theory*, R. M. Dreizler, E. K. U. Gross, Springer Verlag, Berlin **1990**. See also: B. Farid, *J. Phys. Condens. Matter* **1998**, *10*, L1.
[31] a) Gaussian 92/DFT, Revision G, M. J. Frisch, G. W. Trucks, M. Head-Gordon, P. M. W. Gill, M. W. Wong, J. B. Foresman, B. G. Johnson, H. B. Schlegel, M. A. Robb, E. S. Replogle, R. Gomperts, J. L. Andres, K. Raghavachari, J. S. Binkley, C. Gonzalez, R. L. Martin, D. I. Fox, D. J. DeFrees, J. Baker, J. P. Stewart, J. A. Pople, Gaussian, Inc., Pittsburgh **1992**; b) Gaussian 94, Revisions B2, G.2, M. J. Frisch, G. W. Trucks, H. B. Schlegel, P. M. W. Gill, B. G. Johnson, M. A. Robb, J. R. Cheeseman, T. Keith, G. A. Petersson, J. A. Montgomery, K. Raghavachari, M. A. Al-Laham, V. G. Zakrzewski, J. V. Ortiz, J. B. Foresman, C. Y. Peng, P. Y. Ayala, W. Chen, M. W. Wong, J. L. Andres, E. S. Replogle, R. Gomperts, R. L. Martin, D. J. Fox, J. S. Binkley, D. J. Defrees, J. Baker, J. P. Stewart, M. Head-Gordon, C. Gonzalez, and J. A. Pople, Gaussian, Inc., Pittsburgh, **1995**.
[32] a) A. E. Reed, F. Weinhold, *J. Chem. Phys.* **1985**, *83*, 1736; b) A. E. Reed, L. A. Curtiss, F. Weinhold, *Chem. Rev.* **1988**, *88*, 899.
[33] S. Kleinheinz, V. Pfennig, K. Seppelt, *Chem. Eur. J.* **1998**, *4*, 1687.
[34] a) See for example: P. Pyykkö, *Chem. Rev.* **1988**, *88*, 563; b) Compare also: W. Küchle, M. Dolg, H. Stoll, *J. Phys. Chem. A* **1997**, *101*, 7128, and references therein.
[35] B. Krebs, A. Müller, H. Beyer, *J. Chem. Soc. Chem. Commun.* **1968**, 263; B. Krebs, A. Müller, H. Beyer, *Inorg. Chem.* **1969**, *8*, 436.
[36] B. Krebs, *Angew. Chem.* **1969**, *81*, 328; *Angew. Chem. Int. Ed. Engl.* **1969**, *8*, 381; B. Krebs, *Z. Allg. Anorg. Chem.* **1971**, *380*, 146.
[37] A recent DFT study of complexes of $[CH_3MO_3]$ (M = Tc, Re) with nucleophiles came to a different conclusion (S. Köstlmeier, V. A. Nasluzov, W. A. Herrmann, N. Rösch, *Organometallics* **1997**, *16*, 1786). However, this is probably an artefact of the Mulliken population analysis employed.
[38] See for example: *Orbital Interactions in Chemistry*, T. A. Albright, J. K. Burdett, M. Whangbo, Wiley, New York, **1985**.
[39] J. F. Gibson, G. M. Lack, K. Mertis, G. Wilkinson, *J. Chem. Soc. Dalton Trans.* **1976**, 1492.
[40] M. A. Ansari, C. H. Mahler, J. A. Ibers, *Inorg. Chem.* **1989**, *28*, 2669.
[41] V. G. Malkin, O. L. Malkina, M. E. Casida, D. R. Salahub, *J. Am. Chem. Soc.* **1994**, *116*, 5898.
[42] deMon program: D. R. Salahub, R. Fournier, P. Mlynarski, I. Papai, A. St-Amant, J. Ushio in *Density Functional Methods in Chemistry* (Eds.: J. Labanowski, J. Andzelm); Springer, New York **1991**; A. St-Amant, D. R. Salahub, *Chem. Phys. Lett.* **1990**, *169*, 387.
[43] W. Kutzelnigg, U. Fleischer, M. Schindler in *NMR-Basic Principles and Progress, Vol. 23*; Springer, Heidelberg **1990**, pp. 165ff.
[44] M. Kaupp, O. L. Malkina, V. G. Malkin, *J. Chem. Phys.* **1997**, *106*, 9201.
[45] K. Mertis, G. Wilkinson, *J. Chem. Soc. Dalton Trans.* **1976**, 1488.

  0947-6539/98/0409-1686 $ 17.50+.50/0